Rationalizing the Effect of Triethylaluminum on the Cr/SiO2 Phillips Catalysts

Rationalizing the effect of triethylaluminum on the Cr/SiO_2 Phillips catalysts

Giorgia A. Martino,[1] Alessandro Piovano,[1] Caterina Barzan,[1] Jabor Rabeah,[2] Giovanni Agostini,[2,#] Angelika Bruekner,[2] Giuseppe Leone[3], Giorgia Zanchin,[3] Takashi Monoi,[4] and Elena Groppo[1,*]

[1]Department of Chemistry, NIS Centre and INSTM, University of Torino, via G. Quarello 15A, 10135 Torino, Italy
[2] Leibniz Institute for Catalysis at the University of Rostock (LIKAT), Albert-Einstein-Str. 29D-18059 Rostock
[3] CNR-Istituto per lo Studio delle Macromolecole (ISMAC), via A. Corti 12, I-20133 Milano, Italy
[4] R&D Division, Japan Polychem Corporation, 1-1 Marunouchi 1-chome, Chiyoda-ku, 100-8251 Tokyo, Japan
*Corresponding author: elena.groppo@unito.it

Abstract

In contrast to most of the other olefin polymerization catalysts, the Cr/SiO_2 Phillips catalyst does not need any activator to develop its activity. However, it is known that the addition of small amount of metal-alkyls has drastic effects on the catalyst performances and it is one of the strategies involved in the industrial practice to tailor the properties of the produced polyethylene. In this work, we conducted a systematic investigation on the effect of triethylaluminum (TEAl) on the $Cr(VI)/SiO_2$ catalyst, with the ultimate goal to determine the properties of the Cr sites at a molecular level and to correlate them to the properties of the produced polyethylene. To this aim we coupled kinetic tests during the polymerization of ethylene, spectroscopic methods (DR UV-Vis-NIR, EPR, FT-IR of probe molecules) and the polymer characterization. We found that, at an Al:Cr ratio of 2:1, only ca. 50% of the original Cr(VI) sites are reduced, to a variety of species comprising: 1) Cr(IV) bis-alkyl sites, which are probed by CO and are the major actors in the polymerization of ethylene, explaining the faster polymerization initiation rate; 2) 6-fold coordinated Cr(III) sites, which are not accessible by probes and whose amount does not correlate with the catalyst activity; 3) two types of mono-grafted Cr(II) sites, all deriving from the over-reduction of the Cr(IV) bis-alkyl sites, having respectively weak and strong Lewis acid character, the former responsible for in situ α-olefin generation (and hence contributing with the enchainment of short polymer branching), and the latter accounting for the formation of the high M_w polymer fraction.

Overall, our results demonstrate that the catalytic performances of the Cr sites depend not only on the oxidation state, but rather on a combination of molecular structure, acidic character and nature of the ancillary ligands. Hence, by tuning the structure and the acid character of the Cr sites, it is possible to move from a system that essentially affords oligomers from ethylene to one that affords high M_w polymers.

Key-words:

Phillips catalyst, chromium, triethylaluminum, spectroscopies, ethylene polymerization, polyethylene, heterogeneous catalysis

Table of Contents

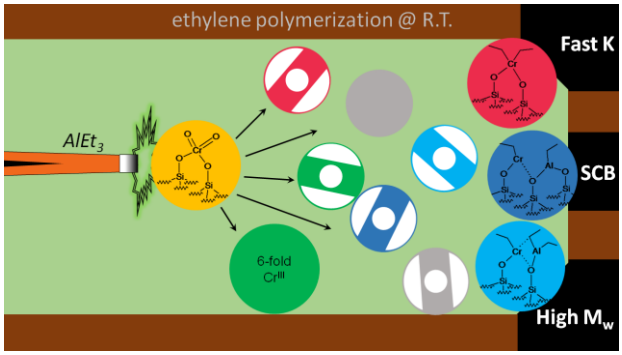

1. Introduction

Since its discovery in 1951,[1] the Cr/SiO_2 Phillips catalyst has a primary role in the production of High Density Polyethylene (HDPE) thanks to its versatility, and the possibility to tailor the polyethylene (PE) properties by slightly changing the catalyst formulation, the activation treatment and/or the polymerization conditions.[2-8] Most of the breakthroughs in this field have been the results of many years of practice in the industrial laboratories, but sometimes also of serendipitous discoveries. This is the case for Lewis acids such as metal-alkyls (e.g. AlR_3, BR_3, MgR_2, ZnR_2 LiR, where R is an alkyl group),[2] whose effect was discovered as a consequence of an accidental contamination in an industrial plant from a polymerization line running Ziegler-Natta catalysts.[9] Indeed, in contrast to the latter that necessitate a co-catalyst for polymerizing olefins, the Phillips catalyst does not need any activator for developing its activity. However, very small amounts of metal-alkyls have drastic effects on the catalyst performance, lowering the induction time necessary to develop the polymerization rate, increasing the activity, improving the H_2 sensitivity for molecular weight (M_w) regulation, promoting the in situ branching, and modifying the active sites distribution.[2] For these reasons, metal-alkyls are nowadays commonly employed in the industrial practice to tailor the catalyst performances.

Some of the effects of metal-alkyls are clear, but their "interaction" at the molecular level with the Cr sites is still unknown, and only some hypotheses have been proposed in the literature, which however still need to be confirmed experimentally.

1) At first, metal-alkyl co-catalysts act as **reducing and alkylating agents**, and this explains the shortening of the induction time and the improved activity. In fact, the reduction and the alkylation of the initial Cr(VI) precursor are considered as the two fundamental and rate-determining steps for developing activity and, in the absence of a co-catalyst, both steps are slowly accomplished by ethylene itself through a still unknown mechanism.[2,10,11] The nature of the active sites initiating the polymerization of ethylene is still under debate and, depending on the catalyst history and the reaction conditions, Cr(II), Cr(III) and Cr(IV) species[2,10,12-23] have been proposed. Similarly, the nature of the Cr sites modified by metal-alkyls is not clarified yet. However, it is generally accepted that they must be reduced and alkylated, so that ethylene can easily undergo insertion into the chromium–alkyl bond.[9,16,24-28]
2) Besides their function as reducing/alkylating agents, the metal-alkyls are known to **modify also the silica surface** by reacting with silanol and/or siloxane groups,[29-33] and as such they can have an indirect impact on the Cr sites, becoming part of the environment of the sites and thus influencing their behavior.[2] However, direct experimental evidence of the proximity of the Cr sites to the Al-containing moieties are very scarce.[34]
3) Moreover, the presence of a metal-alkyl co-catalyst affects the polymer properties, broadening the molecular weight distribution (M_w/M_n), and increasing the branching degree.[2,35-37] According to McDaniel, this influence can be explained primarily by **a change in the active site distribution**.[2] Some sites become active more rapidly in the presence of a co-catalyst, thus increasing their contribution to the polymer M_w/M_n. Still other sites can be activated only in the presence of a co-catalyst, and McDaniel claims that these particular sites produce higher-M_w polymer chains.[2,6] Therefore, the addition of a co-

catalyst often tends to introduce a high-M_w tail in the M_w/M_n. It has been also proposed[2] and demonstrated[38,39] that the metal-alkyls can attack the Cr-support bond, thus converting the initially bis-grafted Cr species into mono-grafted ones, that are known to be responsible for in situ α-olefin generation. However, there are not direct experimental evidences for the existence of these species.

4) Finally, the metal-alkyls are also known to work as **scavengers**, reacting with and removing any poison present at trace levels in the feed streams, particularly oxygen, water, and redox by-products.

The various metal-alkyls probably act in each of these ways to different extent. Moreover, also the co-catalyst stoichiometry has an influence, and it is known that there is an optimal ratio (expressed as the metal co-catalyst-to-Cr mole ratio), different for each co-catalyst, that gives the highest activity. Beyond the optimal co-catalyst concentration, the metal-alkyl can slow down the polymerization rate and even destroy the catalyst. It has been proposed that catalyst destruction occurs through a double attack to the Cr-support bonds, so that the Cr sites are completely detached from the silica surface with the consequent loss in activity.[2]

It is thus clear that, by changing the metal-alkyl and its concentration, it is possible to fine tune the catalyst properties, opening the route to many diversified polymers. Understanding how the metal-alkyl affects the properties of the Cr sites at a molecular level would represent a step further in the design of chromium-based heterogeneous catalysts. The scientific research in this field is still at its infancy. To the best of our knowledge there are only very few works reporting a molecular level investigation of the Cr sites modified by metal-alkyls,[9,16,24-28] and most of them are focused on a single technique that, even when extremely sensitive, may miss other important details. The most recent works are those of Cicmil et al.,[9,27,28] who studied the effect of triethylaluminum (TEAl) on a Cr/SiO_2-TiO_2 catalyst, focusing on the catalyst particle architecture, without however offering a picture of the structure of the modified sites.

The ambitious goal of our work was to investigate the properties at a molecular level of the Cr sites in the $Cr(VI)/SiO_2$ Phillips catalyst after the reaction with TEAl, and to correlate them with the properties of the produced PE. This investigation tuned out to be challenging, because the modifications induced by TEAl further increased the complexity of the catalyst, creating a variety of Cr sites with different oxidation state and the local structure. To this end, we adopted a multi-technique approach, comprising EPR, DR UV-Vis-NIR and FT-IR spectroscopies (the latter also in the presence of probe molecules), since these techniques have been demonstrated to be extremely sensitive, and able to discriminate among Cr sites of different valence state and coordination geometry. Our spectroscopic investigation allowed us to get information, for the first time, on the structure of the Cr sites modified by TEAl at a molecular level. Finally, we tried to correlate each Cr site to a specific function in ethylene conversion, finding a justification for the M_w/M_n of the obtained PE.

2. Experimental

2.1. Catalyst synthesis, activation and modification by TEAl

The Phillips catalysts were prepared by wet-impregnation of the silica support (aerosil, surface area 380 m^2/g) with an aqueous solution of chromic anhydride. It is worth noticing that aerosil is a non-porous, not fragmenting, highly pyrogenic SiO_2 with optimum scattering properties that makes it very suitable for optical spectroscopies. Two different batches of samples with chromium loadings of 0.5 wt% and 1.0 wt were synthetized. The former was used for the DR-UV-Vis-NIR measurements and the latter for FT-IR and EPR spectroscopies and for the kinetics experiments. The choice was done to optimize the spectral quality. Cross-checking experiments demonstrated that, when the activation is properly conducted, the spectroscopic properties are the same irrespective of the Cr loading, as already stated in the past.[10]

The Phillips catalyst was activated according to a procedure optimized during more than 15 years of research in the Torino's group,[10] which involves the following steps: i) evacuation at 650°C (dynamic vacuum, equilibrium pressure below 10^{-4} mbar) followed by calcination in O_2 at the same temperature for 1 hour; ii) evacuation at 350 °C for 30 minutes; and iii) cooling down to room temperature in dynamic vacuum. It was previously demonstrated that step i) provides Cr(VI) sites with preferential mono-chromate structure.[10,11,40] In the following we will call this catalyst as Cr(VI)/SiO_2.

The modification with TEAl was achieved by impregnating the activated samples (either in the form of pellet or in the powder form, depending on the type of measurement) directly in the glove-box with a stoichiometric amount of TEAl diluted in anhydrous hexane, corresponding to an Al:Cr ratio of 2:1, as suggested in the literature.[2,9,16,27,28] In a few cases, the effect of an excess of TEAl was also explored, corresponding to an Al:Cr ratio of 4:1. The resulting catalysts are labelled Cr(VI)/SiO_2+TEAl(2:1) and Cr(VI)/SiO_2+TEAl(4:1), respectively, where the numbers in parenthesis indicate the TEAl concentration expressed as the Al:Cr ratio.

2.2 Spectroscopic methods

Diffuse reflectance (DR) UV-Vis-NIR spectra were collected using a Varian Cary5000 spectrophotometer with a diffuse reflectance accessory. The samples were measured in the form of thick self-supported pellets (surface density of ca. 200 mg/cm^2), placed inside a cell equipped with an optical quartz (suprasil) window that allows performing thermal treatments and measurements in the presence of gases. For identifying changes of the Cr sites during ethylene polymerization, DR UV-Vis-NIR spectra were collected prior and after dosing 200 mbar of ethylene at room temperature for a few minutes. In all the cases, the spectra were collected in reflectance (R%), and the reflectance signal was later converted into Kubelka-Munk values.

Transmission FT-IR spectra were collected at 2 cm^{-1} resolution with a Bruker Vertex70 instrument equipped with a MCT detector. The experiments were performed on samples in the form of thin self-supported pellets (surface density of ca. 30 mg/cm^2), placed inside a quartz cell equipped with two KBr windows, which allows performing thermal treatments and measurements in the presence of gases. All the FT-IR spectra were normalized to the thickness

of the pellet (evaluated from the intensity of the absorption bands due to the silica support), in order to allow quantitative comparisons to be done.

For probing the accessible Cr sites after modification with TEAl, FT-IR experiments of adsorbed carbon monoxide (CO) and d-acetonitrile (CD_3CN) were performed. CO was dosed in the gas phase (equilibrium pressure P_{CO} = 100 mbar) at room temperature. CD_3CN was dosed in the vapor phase (from the liquid vapor tension, equilibrium pressure P_{CD3CN} = 20 mbar) at room temperature. A FT-IR spectrum was collected at the maximum CO (or CD_3CN) coverage, followed by systematic expansions of the gas in the vacuum line to diminish the equilibrium pressure in a controlled way. FT-IR spectra were collected at each expansion, until no more changes were observed (irreversibly adsorbed fraction).

EPR spectra were recorded on a Bruker EMX CW-micro X-band EPR spectrometer equipped with an ER4119HS high-sensitivity resonator, with a microwave power of Ca 6.9 mW and modulation frequency and amplitude of 100 kHz and up to 5 G, respectively. The EPR spectrometer was equipped with a temperature controller and liquid N_2 cryostat for low temperature measurements. The $h\nu = g\beta B_0$ equation was used to calculate g values with ν and B_0 being the frequency and resonance field, respectively. g values Calibration was performed using 2,2-Diphenyl-1-picrylhydrazyl as a standard (g = 2.0036 ± 0.0004).

Generally for the EPR measurements, about 50 mg of the calcined Cr/SiO_2 catalyst was placed in a special homemade EPR tube, calcined again in situ at 650 °C in O_2 and evacuated before EPR measurements. The TEAl-modified $Cr(VI)/SiO_2$ catalyst was prepared by impregnation of the Cr/SiO_2 catalyst inside the EPR tube with a solution of TEAl in heptane, under Ar atmosphere inside a glove box, followed by evacuation prior the EPR measurement. To investigate the changes of the Cr sites during ethylene polymerization, the catalyst was in situ exposed to ethylene (100 mbar) at room temperature for a few minutes, followed by evacuation. The EPR spectra were recorded after ethylene polymerization at 100 and 293 K.

2.3 Polymerization tests and analysis of the polymer

The kinetics of gas-phase ethylene polymerization were evaluated in mild conditions, by sending 200 mbar of ethylene at room temperature over 0.3 g of catalyst (both without and with modification by TEAl) inside a quartz reactor of known volume, and recording the ethylene pressure as a function of time, as reported elsewhere.[41] The kinetic constant k was determined considering the first order kinetic law $dP(C_2H_4)/dt = kP(C_2H_4)n_{Cr}$, where k is the kinetic constant (in $mol_{Cr}^{-1}s^{-1}$) and n_{Cr} is the number of Cr moles in the catalyst. By integrating the previous equation it turns out that $lnP(C_2H_4) = kn_{Cr}t$. Hence, by plotting $lnP(C_2H_4)$ as a function of time t, it is possible to determine k as the slope of the obtained line, once that n_{Cr} is known.

In order to give insight into the catalytic process and properties, all the polymers obtained were fully characterized with the aid of different techniques, to determine the polymer properties. The molecular weight average (M_w) and the molecular weight distribution (M_w/M_n) of the polymers were determined by a high temperature Waters GPCV2000 size exclusion chromatography (SEC) system equipped with a refractometer detector. The experimental conditions consisted of three PL Gel Olexis columns, *ortho*-dichlorobenzene as the

mobile phase, 0.8 mL min^{-1} flow rate, and 145 °C temperature. The calibration of the SEC system was constructed using eighteen narrow M_w/M_n poly(styrene) standards with molar weights ranging from 162 to 5.6×10^6 g mol^{-1}. For SEC analysis, about 12 mg of polymer was dissolved in 5 mL of *ortho*-dichlorobenzene with 0.05% of BHT as antioxidant.

Differential scanning calorimetry (DSC) scans were carried out on a Perkin-Elmer DSC 8000 instrument equipped with a liquid sub-ambient device under nitrogen atmosphere. The sample, typically 5 mg, was placed in a sealed aluminum pan, and the measurement was carried out from −30 to 180 °C using heating and cooling rate of 20 °C min^{-1}. T_m and ΔH_m values were recorded during the second heating. Crystallinity (X) was calculated from the DSC scans as follows: $X_{DSC} = (\Delta H_f/\Delta H_0)\times100$, where ΔH_f is the enthalpy associated with the melting of the sample and ΔH_0 is the melting enthalpy of a 100% crystalline poly(ethylene) taken equal to 290 J g^{-1}.

Wide-angle X-ray diffraction (XRD) experiments were performed at 25°C under nitrogen flux, using Siemens D-500 diffractometer equipped with Soller slits (2°) placed before sample, 0.3° aperture and divergence windows, and VORTEX detector with extreme energy resolution specific for thinner films. CuKα radiation with, power used 40 KV x 40 mA was adopted, each spectrum was carried out with steps of 0.05 °2θ, and 6s measure time.

3. Results

3.1. Effect of TEAl on ethylene polymerization and properties of the obtained polyethylene

The performances of Cr(VI)/SiO_2+TEAl(2:1) in gas-phase ethylene polymerization were initially evaluated under mild conditions. Figure 1a shows the decrease of ethylene pressure over time for TEAl-modified Cr(VI)/SiO_2 catalyst at room temperature, compared to bare Cr(VI)/SiO_2 at 150 °C.[42] It is evident that TEAl dramatically influences the ethylene polymerization kinetic, eliminating the induction time and rising the polymerization rate. The polymerization rate was evaluated in the approximation of a first order reaction,[43] taking into account only the first minute of reaction (as described in the Experimental section). The rate constant *k* for the TEAl-modified catalyst was estimated to be ca. 140 s^{-1}mol Cr^{-1}, that is ca. 20 times higher than that of the parent Cr(VI)/SiO_2 evaluated in similar conditions (ca. 8 s^{-1}mol Cr^{-1}). It is worth noticing that the rate constant does not significantly change when the double of TEAl is used (Al:Cr = 4:1, *k* of ca. 150 s^{-1}molCr^{-1}) (Figure S1), in good agreement with the literature data.[2] In both cases, the reaction rate decreases after the first minutes of reaction, denoting a progressive catalyst deactivation, likely associated to the absence of fragmentation in pyrogenic silica, and the consequent limitation in diffusional ethylene mobility.

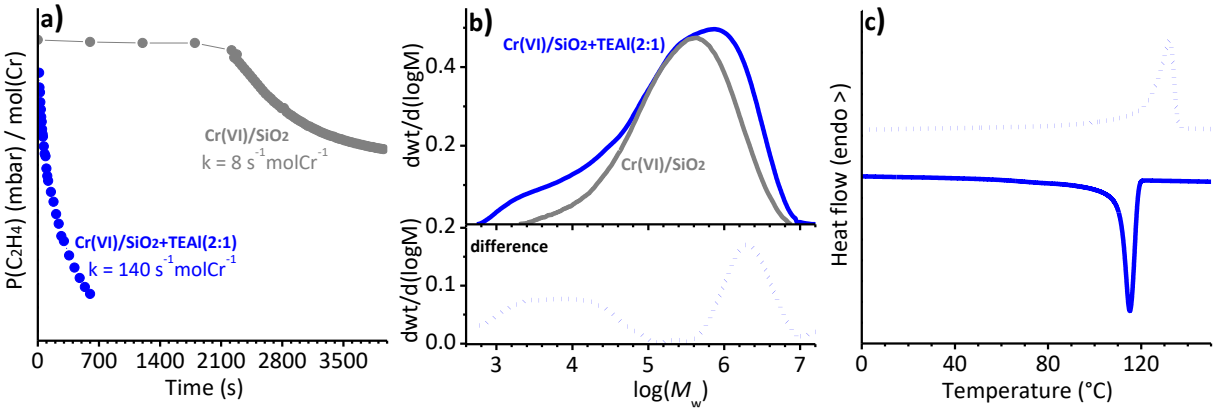

Figure 1. Part a): Kinetics of the gas-phase ethylene polymerization on the Cr(VI)/SiO_2 catalyst in comparison to that on Cr(VI)/SiO_2+TEAl(2:1). Part b) SEC trace of the PE obtained over Cr(VI)/SiO_2 and Cr(VI)/SiO_2+TEAl(2:1) and their difference. Part c) DSC profile of the PE obtained over Cr(VI)/SiO_2+TEAl(2:1).

The obtained PE was analyzed by SEC (Figure 1b), DSC (Figure 1c), and XRD (Figure S2). In Figure 1b, the SEC trace of PE obtained with TEAl-modified Cr(VI)/SiO_2 is shown together with that of PE from unmodified Cr(VI)/SiO_2. The average M_w (7.75×10^5 g mol^{-1}) of PE obtained with TEAl-modified Cr(VI)/SiO_2 is remarkably higher than that of PE from unmodified Cr(VI)/SiO_2 (typically 3.0×10^5 g mol^{-1}). In addition, the SEC curve exhibits an asymmetric shape with a pronounced shoulder at high M_w and a low-M_w tail in the molecular weight distribution respectively. Therefore, the addition of the Al-cocatalyst introduce a high- and a low-M_w contribution in the polymer M_w distribution. This accounts for the rise in the M_w/M_n (M_w/M_n = 30) compared to the PE obtained with unmodified Cr(VI)/SiO_2 ($M_w/M_n \approx 10$).[2,3] The broad M_w/M_n is a clear indication that the catalyst contains a large variety of active sites, some of them responsible for the low-M_w fraction, and some others for the high-M_w fraction. The fact that the M_w/M_n is broader for PE obtained using TEAl is a further indication that the active

species involved in the polymerization may be even more (and different from each other), and thus their "description" even more complex.

The heating DSC trace shows a relative sharp melting event followed by a wide tail that spans the temperature range up to 80 °C. The melting temperature (T_m) taken at the maximum peak is 132 °C, while the enthalpy of fusion (ΔH_m) is 155 J g^{-1}, corresponding to a bulk crystallinity of about 53%, in good agreement with the crystallinity calculated by XRD (50%, Figure S2). The cooling DSC trace shows a sharp crystallization exotherm, suggesting that the PE lamellae are homogeneously packed, with a maximum at about 115 °C. Moreover, from these data we can rule out the presence of some short chain branches, contributing to the bulk reduced crystallinity and to the relatively low melting temperature despite the polymer has a high M_w. It is worth noting that a more detailed microstructure determination to establish the degree and type of branches via NMR spectroscopy was unfeasible because of the low solubility of the polymer.

3.2. Spectroscopic investigation of Cr(VI)/SiO_2 modified by TEAl

The reaction of Cr(VI)/SiO_2 with TEAl was initially monitored by FT-IR spectroscopy (Figure 2a). The spectrum of the oxidized catalyst (spectrum 1) is dominated by the features of a highly dehydroxylated silica, with the characteristic band of free silanols at 3748 cm^{-1} (Figure 2a'), the silica framework modes below 1250 cm^{-1}, and their overtones in the 2100-1500 cm^{-1} range. The presence of the chromates at the silica surface is revealed by the very weak band at 1980 cm^{-1} (Figure 2a''), which was attributed to the first overtone of the v(Cr=O) vibrational mode.[10,40,41,44,45]

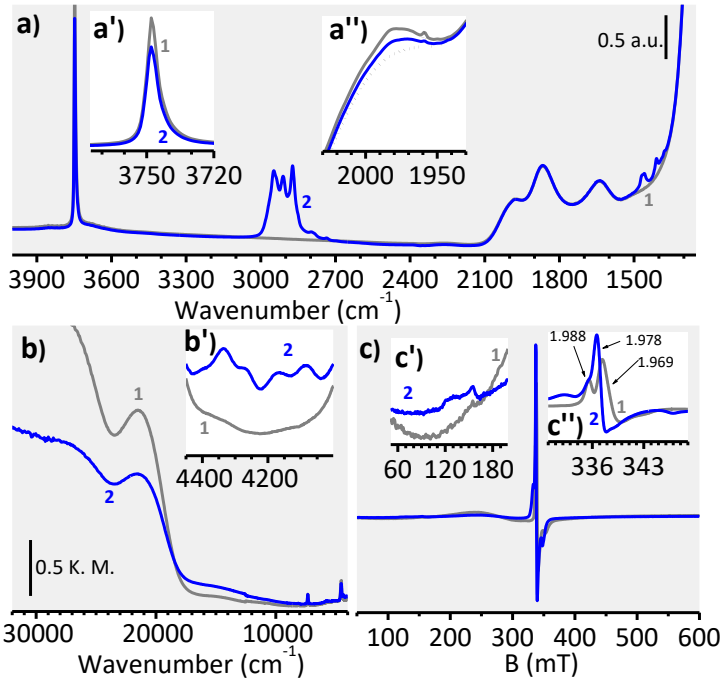

Figure 2. FT-IR (part a), DR UV-Vis-NIR (part b) and X-band EPR (part c) spectra of Cr(VI)/SiO_2 (spectra 1) and of Cr(VI)/SiO_2+TEAl(2:1) (spectra 2). The insets show a magnification of: a') the v(Si-OH) vibrational region; a'') the vibrational region characteristic of monochromates (first overtone of the v(Cr=O) vibrational mode); b') the NIR region, where the overtones and combination of the v(CH_x) appear; c') and c'') mid- and low-field regions in EPR spectra. In inset a'') the spectrum of SiO_2 activated in the same conditions is shown for comparison (dotted).

The reaction of Cr(VI)/SiO_2 with TEAl (spectrum 2) is demonstrated by the appearance of several absorption bands in the 3000-2800 cm^{-1} and 1500-1300 cm^{-1} regions, which are due to the typical stretching and bending modes of the CH_x moieties in Al-alkyl compounds.[46] At the same time, the absorption band at ca. 3750 cm^{-1}, due to the surface OH groups, is slightly affected in intensity (Figure 2a'), demonstrating that TEAl reacts with a fraction of the silanol groups. According to the literature,[29-33] the reaction leads to the formation of mono-grafted ≡SiO-AlR_2 species and the release of RH (path 1 in Scheme S1). It has been demonstrated[29-33] that TEAl reacts also with the siloxane bridges present at the surface of highly dehydroxylated silica (paths 2 and 3 in Scheme S1), leading to the formation of mono grafted ≡SiO-AlR_2 species (path 2) that, upon further reaction with a vicinal siloxane group (path 3), would lead to the formation of a bis-grafted $(≡SiO)_2$-AlR species. All these surface species contribute to the FT-IR spectrum in the CH_x vibrational modes, but they are not distinguishable. Finally, TEAl reacts also with chromates, as testified by the decrease of the band at 1980 cm^{-1} (Figure 2a''). By roughly evaluating the integrated area of this band, we can estimate that ca. 50% of the original chromates are reduced (and likely alkylated) in these conditions, with the concomitant production of $Al(OR)_xR_y$ by-products. This value is in good agreement with the XPS results reported by Liu et al.,[16] who found that ca. 55% of the chromates remain unreduced in similar conditions, and is also consistent with previous observations that TEAl does not go deep inside the catalyst particle.[47] However, FT-IR spectroscopy does not allow to characterize neither the reaction by-products nor the modified Cr sites. For this reason, we turned our attention to two complementary techniques that are sensitive to the electronic and magnetic properties of the Cr sites, namely DR UV-Vis-NIR and EPR spectroscopies.

Previous works demonstrated that after the oxidative treatment at 650 °C, most of the Cr sites are in the form of monochromates.[10,11,40,48] These species have a characteristic DR UV-Vis spectrum (spectrum 1 in Figure 2b), with intense bands at about 39500, 29000 and 21200 cm^{-1}, which are assigned to O → Cr(VI) charge-transfer transitions.[10,11,40,48-51] Cr(VI) sites, which have a d^0 electronic configuration, are diamagnetic, and hence EPR silent. Nevertheless, a pseudo axial resonance in the 1.895-1.979 *g* region is observed in the X-band EPR spectrum of Cr(VI)/SiO_2 (spectrum 1 in Figure 2c), which is due to a small amount of Cr(V) species, detected in the X-band EPR spectra of Cr(VI)/SiO_2 since the early 1990s[48,52-57] and usually considered as spectators. The amount of Cr(V) is typically lower than 2% of the total Cr sites.[56]

After reaction with TEAl, the EPR signal of Cr(V) becomes sharper and slightly shifts to g = 1.978 (spectrum 2 in Figure 2c''), likely as a consequence of the proximity of TEAl (or its reaction by-products) to the Cr(V) sites, that causes a modification of their symmetry. However, we cannot completely rule out that part of the Cr(VI) are reduced to Cr(V) by TEAl. No additional bands are observed in the EPR spectrum, but only an extremely weak signal at g = 4.3 (spectrum 2 in Figure 2c'), which indicates the presence of a tiny amount of isolated, strongly distorted, Cr(III) sites, in good agreement with the XPS data reported by Liu et al.,[16] who estimated ca. 2% of Cr(III) sites in similar conditions. This suggests that the majority of the Cr(VI) sites is reduced by TEAl to Cr species which are EPR silent, either Cr(IV) or Cr(II). It is worth noticing that the EPR signal related to the isolated Cr(III) sites increases when twice the

amount of TEAl is used (Figure S3), while the catalytic activity is almost unaffected (Figure S1). This suggests that the presence of Cr(III) sites does not correlate with the catalytic activity.

On the other hand, upon interaction of Cr(VI)/SiO_2 with TEAl the color of the catalyst changes from orange-yellow to brown-greenish. Correspondingly, the intense bands at 21200, 29000 and 39500 cm^{-1} in the DR UV-Vis-NIR spectrum decrease in intensity (spectrum 2 in Figure 2b), accompanied by the appearance of i) a broad and weak band covering the whole 8000-20000 cm^{-1} range, i.e. the region of d-d transitions for reduced chromium species, and ii) a complex envelope of bands in the NIR region, assigned to the overtones and the combinations of the $\nu(CH_x)$ and $\delta(CH_x)$ vibrational modes of the alkyl groups deriving from TEAl. Going into more detail, the band at 21200 cm^{-1} (attributed to the monochromates) decreases in intensity by ca. 30% (i.e. less than expected on the basis of the FT-IR results, which suggested that ca. 50% of the original chromates are reduced by TEAl), slightly shifts to lower wavenumber (at about 20600 cm^{-1}) and becomes broader. To better appreciate the shift, the same spectra are reported in terms of second derivative in Figure S4. These observations might suggest that a fraction of Cr(VI) sites has been reduced and alkylated to Cr(IV)$-(CH_2CH_3)_2$ sites, which are among the possible Cr species proposed by McDaniel to be present after modification with TEAl.[2] Indeed, the UV-Vis spectrum of Cr(IV)-alkyls typically has two bands around 18000 and 20500 cm^{-1},[58] that converge into a broad band centered right around 21000 cm^{-1} after grafting onto a dehydroxylated silica.[59] As far as the assignment of the broad d-d band is concerned, both Cr(II) and Cr(III) species with different geometry might contribute to this spectral range. The only message that can be safely extracted comes from the rather weak intensity of this band, which suggests that the reduced Cr sites should have prevalently a 6-fold coordination irrespective of their oxidation state. Indeed, d-d transitions are formally Laporte forbidden for transition metals in octahedral symmetry.

Summarizing, the whole series of spectroscopic data reported in Figure 2 indicate that TEAl reduces ca. 50% of chromates to a variety of reduced Cr sites, possibly including Cr(IV)-alkyls and 6-fold coordinated Cr(III) and Cr(II) species. The coordination sphere of the reduced Cr sites is at least partially defined by the ≡SiO-Al$(CH_2CH_3)_2$ (and similar) moieties which derive from the reaction of TEAl with the silica surface.

3.3 The accessibility of the Cr sites modified by TEAl.

Successively, the accessibility of the reduced Cr sites in Cr(VI)/SiO_2+TEAl(2:1) was investigated by means of FT-IR spectroscopy of adsorbed probe molecules. CO and CD_3CN were selected as suitable probes since they interact in different ways with the metal sites, thus giving complementary information. In particular, FT-IR spectroscopy of adsorbed CO has been used since decades to characterize the Phillips catalysts,[10,11,40,60] and it has been demonstrated to be one of the most sensitive techniques to the local geometry of the Cr(II) sites. CD_3CN has been often used as a probe for the characterization of acid or basic sites on the surface of different metal oxides,[61-67] but it has never been employed for investigating the Phillips catalyst until our recent work.[34]

3.3.1 Probing the Cr sites with CO

Figure 3a shows the FT-IR spectrum, in the 2040 – 1850 cm^{-1} region, of CO adsorbed at room temperature on Cr(VI)/SiO_2+TEAl(2:1) (spectrum 1). The spectrum is dominated by a main absorption band centered at about 1988 cm^{-1}, with a shoulder at 2024 cm^{-1}. Interestingly, the shape and the position of these bands are very similar to those observed in the spectrum of CO adsorbed on Cr(II)/SiO_2 modified with other co-catalysts, such as triethylsilane (TES)[38,39] or diethylaluminoethoxide (DEALE),[34] two systems recently studied by our group, where the role of the co-catalyst was to change the local geometry of the Cr(II) sites but not their oxidation state. No bands are detected in the spectral region where we should observe the ν(CO) bands of carbonyls formed on highly uncoordinated Cr(II)[10,11,40,60] and Cr(III)[19] sites bis- or tris-grafted on silica (2200 – 2150 cm^{-1}, not shown for clarity), while a couple of very weak bands is detected at 1743 and 1665 cm^{-1} (Figure 3b).

Starting the discussion from the most intense bands (Figure 3a), the interactions of CO with a transition metal site is dominated by either a σ-donation or a π-back-donation contribution, depending on the type, coordination and oxidation state of the metal site.[60] The predominance of the σ-dative contribution causes a blue-shift of ν(CO) with respect to the frequency of the free gas (2143 cm^{-1}), while the π-back-donation causes a red-shift of ν(CO). We have already demonstrated that ν(CO) bands in the 2050 – 1950 cm^{-1} range have to be attributed to CO adsorbed on mono-grafted ≡Si-O-Cr(II)-L species,[11] where the ligand L depends on the type of system. For example, for Cr(II)/SiO_2 modified by TES, L = -$OSiR_3$,[39] while for Cr(II) modified by DEALE, L = alkyl or alkoxy groups.[34] These mono-grafted Cr(II) sites have been proposed to be formed as a consequence of the co-catalyst attack to one of the Cr-O-Si anchoring links and have been advocated as responsible for the in situ α-olefins generation.[2] Hence, the FT-IR spectrum reported in Figure 3a demonstrates that a fraction of the reduced Cr sites in Cr(VI)/SiO_2+TEAl(2:1) is in the form of mono-grafted Cr(II) species, likely stabilized by the ≡SiO-AlR_2 (or similar) species which are present at the silica surface.

We performed an analogous experiment with a 1:1 isotopic mixture of ^{12}CO:^{13}CO, and with pure ^{13}CO. The use of isotopic mixtures is a widely employed method for assigning complex IR spectra, since it allows to decouple two or more CO molecules adsorbed on the same site.[68] When ^{13}CO is used instead of ^{12}CO (spectrum 3 in Figure 3), the two absorption bands at 2024 and 1988 cm^{-1} are isotopically red-shifted by the theoretical 0.9777 factor based on the Hooke law (ν(^{13}CO) = 1975 and 1945 cm^{-1}). A weak absorption band at 1913 cm^{-1} is also present and assigned to $^{12}C^{18}O$ traces in the ^{13}CO feed. The IR spectrum of the ^{12}CO:^{13}CO mixture (spectrum 2 in Figure 3) can be deconvoluted in terms of six components: i) the doublet observed for carbonyl species of pure ^{12}CO (2024-1988 cm^{-1}); ii) the doublet observed for carbonyl species of pure ^{13}CO (1975-1945 cm^{-1}); iii) two singlets at 2009 and 1960 cm^{-1} that fall exactly in the barycenter of the two aforementioned doublets. This IR absorption pattern is typical of di-carbonyl species. In fact, in a di-carbonyl of pure ^{12}CO (or ^{13}CO) the two CO molecules behave as coupled oscillators and the corresponding FT-IR spectrum is characterized by a doublet due to the asymmetric and symmetric vibrations. In the mixed (^{12}CO)(^{13}CO) di-carbonyl the two CO molecules behave as two decoupled mono-carbonyls, giving rise to two distinct bands approximately at the barycenter of the previously discussed doublets.[39,68] Hence,

the FT-IR experiment performed with the ^{12}CO:^{13}CO isotopic mixture demonstrates that the mono-grafted Cr(II) sites are able to form a di-carbonyl species at room temperature, meaning that they have at least vacant coordination sites available. In this respect, it must be noticed that coordination of CO might occur to the expenses of weaker ligands, such as the ≡SiO-AlR_2 (or similar) species nearby.

We also tried to quantify the relative amount of mono-grafted Cr(II) sites with respect to the total Cr sites. In this respect, we compared the integrated intensity of the ν(CO) band for CO on Cr(VI)/SiO_2+TEAl(2:1) to that obtained for Cr(II)/SiO_2+TES, where we previously demonstrated that ca. 85% of the original Cr(II) sites were converted from bis-grafted to mono-grafted.[39] This method allows concluding that ca. 28% of the total Cr(VI) sites were converted by TEAl to mono-grafted Cr(II) sites. This fraction increased to ca. 60% when the amount of TEAl was doubled (Figure S5a).

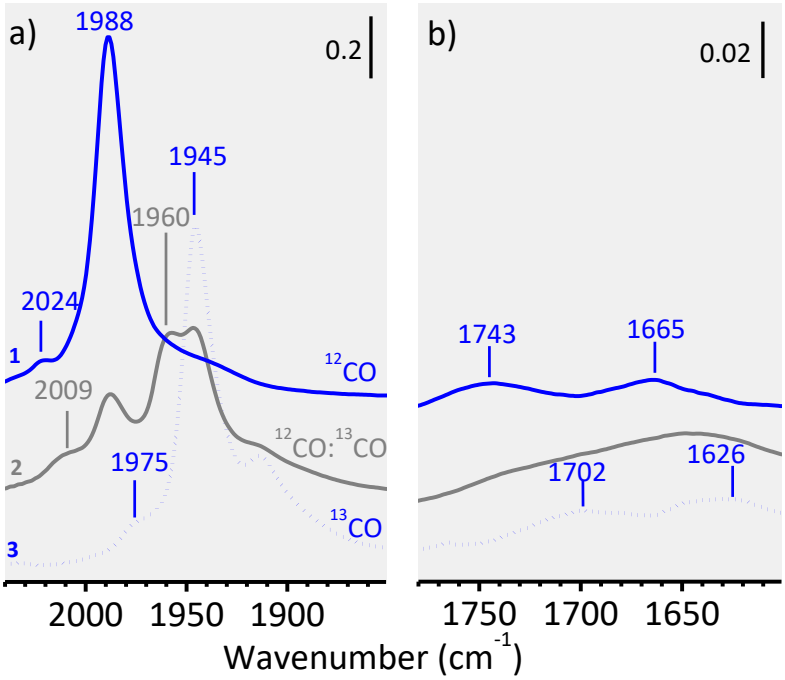

Figure 3. FT-IR spectra of Cr(VI)/SiO_2+TEAl(2:1) in interaction with: i) ^{12}CO (spectrum 1); ii) a 1:1 isotopic mixture of ^{12}CO:^{13}CO (spectrum 2); and iii) ^{13}CO (spectrum 3). The spectra are normalized for the thickness of the pellet (evaluated from the intensity of the bands due to the silica support) and for the CO equilibrium pressure, hence the absolute intensities are comparable. The spectra are vertically shifted for clarity. Part a) shows the ν(C≡O) region of CO coordinated to reduced Cr sites, while part b) shows the to ν(C=O) region of Cr η^1-acyl complexes, which are formed by insertion of CO into a Cr-alkyl bond.

As far as the weak bands in the 1750 – 1600 cm^{-1} range are concerned (Figure 3b), they are tentatively ascribed to ν(C=O) of Cr η^1-acyl complexes, which are formed by insertion of CO into a Cr-alkyl bond. In fact, it is known that η^1-ligands like CO have the tendency to insert into a metal-carbon bond and the acyl ν(C=O) frequencies typically range from 1700 to 1600 cm^{-1}.[69-72] The assignment is corroborated by the observed isotopic shift in the presence of ^{13}CO. Hence, the presence of the two bands at 1743 and 1665 cm^{-1} in the spectrum of CO adsorbed on Cr(VI)/SiO_2+TEA(2:1) indirectly demonstrates that a fraction of the Cr(VI) sites are alkylated by TEAl. Most probably, these are the Cr(IV)–$(CH_2CH_3)_2$ bisalkyl species that have been

hypothesized on the basis of DR UV-Vis spectroscopy, although we cannot exclude that the few Cr(III) species detected by EPR are also alkylated. Notably, the intensity of these bands slightly increases for CO adsorbed on Cr(VI)/SiO_2+TEA(4:1) (Figure S5b), although they do not double, as observed for the band at 1988 cm^{-1}. This indicates that an Al:Cr ratio higher than 2 generates mostly mono-grafted Cr(II) sites.

3.3.2 Probing the Cr sites with CD_3CN

CD_3CN has a basic character stronger than CO, hence it is more sensible to the acidic strength of the adsorption sites. Since both Cr and Al sites are Lewis acids (i.e. prone to accept electrons), acetonitrile is expected to interact with both of them as a soft Lewis base by sharing the nitrogen lone-pair. Because of this interaction, the ν(C≡N) vibration is expected to increase with respect to the free molecule (2267 cm^{-1}) proportionally to the strength of the Lewis acid-base couple. In general, d-acetonitrile is employed to avoid the occurrence of an annoying Fermi resonance effect.[61]

The spectra of CD_3CN adsorbed at room temperature on Cr(VI)/SiO_2+TEAl(2:1) are shown in Figure 4. They are characterized by a complex series of bands that behave differently as a function of the CD_3CN coverage. The two bands at 2276 and 2265 cm^{-1}, which decrease quickly upon degassing, are assigned to CD_3CN adsorbed on the hydroxyls present on the silica surface, and to physisorbed CD_3CN, respectively.[62-65] These bands are the only ones observed for CD_3CN adsorbed on silica dehydroxylated at high temperature,[34] and also for CD_3CN adsorbed on Cr(VI)/SiO_2 (Figure S6a). A second set of bands centered at ca. 2317 cm^{-1} is almost irreversible upon degassing at room temperature, denoting CD_3CN strongly adsorbed to different Lewis acid (LA) sites. At lower CD_3CN coverage, this band is clearly asymmetric, with a maximum at 2317 cm^{-1} and a shoulder at 2305 cm^{-1}. Both Al(III) and Cr(II) sites might contribute to this band. As a matter of fact, when the same experiment is performed on a silica treated with the same amount of TEAl as in Cr(VI)/SiO_2+TEAl(2:1), a very intense and symmetric band is observed at 2317 cm^{-1} (Figure S6b). In contrast, when the same experiment is performed on Cr(II)/SiO_2 (where bis-grafted Cr(II) sites are present), a single band is observed at 2305 cm^{-1} (Figure S6c). Both bands were observed for CD_3CN on Cr(II)/SiO_2+DEALE(2:1), and ascribed to CD_3CN adsorbed on unmodified Cr(II) sites (2305 cm^{-1}) and on Cr(II) sites modified by DEALE and in close proximity of an acidic Al(III) site (2317 cm^{-1}).[34] Hence, Al(III) sites are stronger LA sites than highly uncoordinated Cr(II) species (i.e. the shift of ν(C≡N) is larger with respect to the gas phase), but there might be also modified Cr sites characterized by a similar acidity.

We also repeated the same experiment on a Cr(II)/SiO_2 modified by TES (Figure S6d), where 85% of the originally bis-grafted Cr(II) sites are transformed into mono-grafted ≡Si-O-Cr(II)-L species.[39] Curiously, a symmetric band centered at 2305 cm^{-1} is observed also in this case. This means that CD_3CN is not able to discriminate between bis-grafted Cr(II) sites and mono-grafted ≡Si-O-Cr(II)-L sites, which appear both as LA sites with the same strength. This differentiates CD_3CN from CO, which in contrast is sensitive to the Cr(II) molecular structure. The is due to the different type of interaction between Cr(II) and the two probe molecules. For CD_3CN, the interaction is mainly of acid-base type. CD_3CN is an electron donor and its donation ability rises with the tendency of the adsorbing site to accept electrons, that is with its LA strength. Hence, CD_3CN discriminates the adsorbing sites in terms of their acidity. In contrast,

the interaction of CO with Cr(II) sites is driven by the overlap of its frontier molecular orbitals with specific atomic orbitals of Cr having the right geometry and electronic occupancy. Since atomic orbitals of an adsorption site depend on its local structure and their electronic occupancy is a function of the oxidation state, CO is highly sensitive to both parameters.

Finally, a broad band is observed at ca. 2250 cm^{-1}, which is more visible at low CD_3CN coverage. The low frequency of the ν(C≡N) band suggests a bridging coordination mode for CD_3CN, in analogy to what observed for other ligands.[60] Hence, this band is tentatively ascribed to CD_3CN *bridged* in between Cr(II) and Al(III), indicating the presence of Cr(II)···Al(III) bimetallic species simultaneously probed by the same CD_3CN molecule. It is worth noticing that these sites are likely the most acidic, since they originate from the cooperation of two strong LA sites, and that the low frequency of the corresponding ν(C≡N) band is due to the bridging coordination mode.

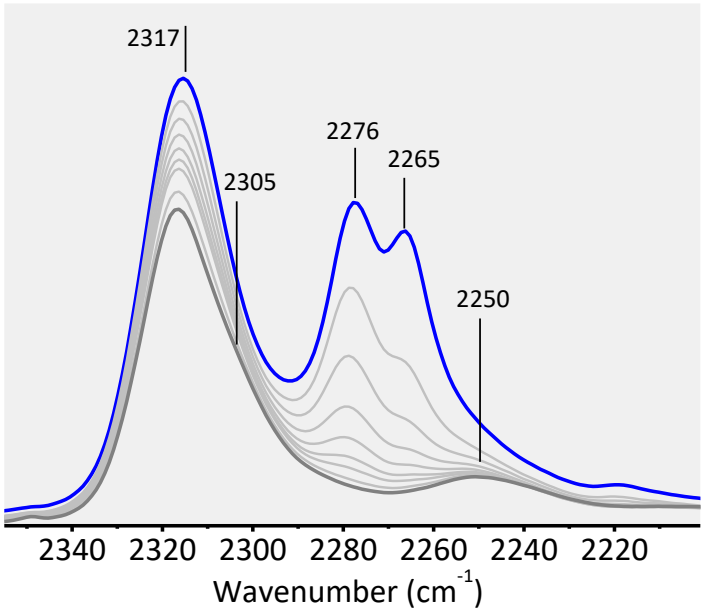

Figure 4. Evolution of the FT-IR spectra, in the $\tilde{\nu}$(C≡N) region, for CD_3CN adsorbed at room temperature on Cr(VI)/SiO_2+TEAl(2:1) catalyst as a function of the CD_3CN coverage (blue: maximum coverage, dark grey: irreversible fraction of CD_3CN, light grey: intermediate coverages).

In summary, CD_3CN probes three different types of acid sites on Cr(VI)/SiO_2+TEAl(2:1): i) weak LA sites (W-LA) (band at 2305 cm^{-1}), which are likely the same mono-grafted ≡Si-O-Cr(II)-L sites probed by CO at 1988 cm^{-1}; ii) strong LA sites (band at 2317 cm^{-1}), which are coordinatively unsaturated Al(III) sites belonging to the –$OAlR_x$ moieties at the silica surface, but can also be a fraction of mono-grafted ≡Si-O-Cr(II)-L sites in close proximity to an Al(III), which however are not able to bridge the CD_3CN probe; and iii) Cr(II)···Al(III) couples (band at 2250 cm^{-1}) at sufficiently close proximity to bind the same CD_3CN molecule in a bridge fashion, that behave as very strong LA sites. It is worth noticing that both the Al(III) sites and the Cr(II)-Al(III) couples were not detected by CD_3CN for Cr(II)/SiO_2 modified by DEALE.[34] We explain this difference on account of the presence of an –OR group in DEALE, that probably promotes the formation of aluminoxane clusters at the silica surface (hence the Al(III) sites are not accessible), and that will interpose between the Cr(II) and the Al(III) sites in the Cr(II)-Al(III) couples (thus hampering

CD_3CN to bind in a bridged fashion). In that case, two types of mono-grafted Cr(II) sites were detected, characterized by a different acid strength, the stronger LA sites being those in proximity of an Al(III) site.

3.4. Identification of the Cr sites involved in ethylene polymerization

Finally, the polymerization of ethylene under mild conditions by Cr(VI)/SiO_2+TEAl(2:1) at the initial stage was monitored by means of DR UV-Vis and EPR spectroscopies (Figure 5). Upon ethylene dosage, the DR UV-Vis-NIR spectra immediately change (Figure 5a). The band at 21060 cm^{-1} is the most affected, while the broad band in the d-d transition region remains almost unaltered. The polymerization of ethylene is demonstrated by the appearance of weak and narrow bands in the 4500-4000 cm^{-1} region, which are due to the overtones and combinations of the stretching and bending vibrational modes of PE (Figure 5a'). According to the discussion above, the band at 21060 cm^{-1} might be due to residual Cr(VI) sites not reduced by TEAl, or to alkylated Cr(IV) sites. The rapid decrease of this band during the polymerization of ethylene supports the second hypothesis. Indeed, ethylene does not reduce the Cr(VI) sites at room temperature. Moreover, we have previously demonstrated that the formation of PE during the first stages of the reaction causes the rapid decrease of the UV-Vis spectroscopic fingerprints of the active sites, while the bands due to spectators (or to Cr sites that initiate the polymerization more slowly) remain unaltered.[12] This is due to the fact that PE forms a white coating around the catalyst particles, which diffuses the incident light and shields the Cr sites involved in the ethylene polymerization from the DR UV-Vis measurements. Hence, the DR UV-Vis data seem to suggest that alkylated Cr(IV) sites are those mostly involved in ethylene polymerization.

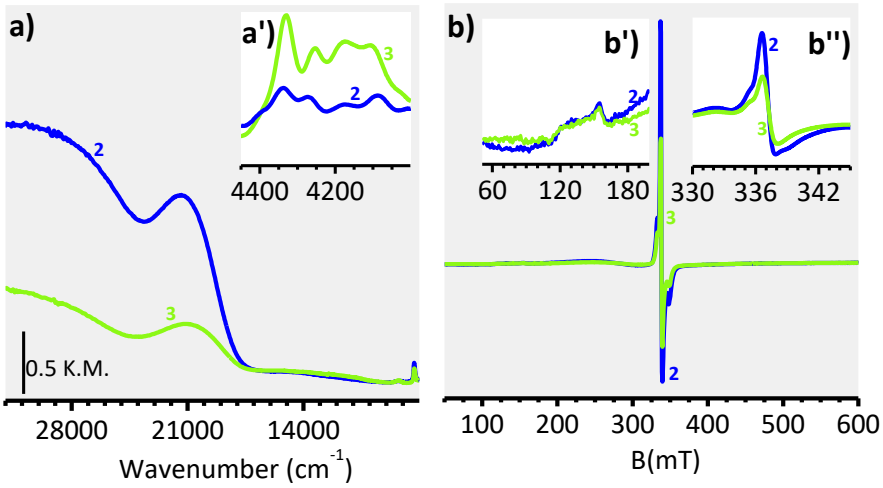

Figure 5. Part a) Evolution of the DR UV-Vis-NIR spectra upon ethylene reaction at room temperature on the Cr(VI)/SiO_2+TEAl(2:1) catalyst (from spectrum 2 to spectrum 3). The inset shows a magnification of the NIR region. Part b) X-band CW-EPR spectra of the Cr(VI)/SiO_2+TEAl(2:1) before (spectrum blue) and after reaction with ethylene at room temperature (spectrum green).

The same experiment was followed by EPR spectroscopy (Figure 5b). Ethylene was admitted on the catalyst at room temperature and the polymerization reaction was quenched after two minutes with liquid nitrogen, followed by collection of the EPR spectrum at 100 K. The polymerization of ethylene was confirmed *a posteriori* by collecting the ATR spectrum of the

powder, which shows the distinctive bands due to PE. The EPR spectrum of Cr(VI)/SiO_2+TEAl(2:1) catalyst is almost unperturbed after ethylene polymerization. In particular, the weak signal at g = 4.3 (Figure 5b'), assigned to a tiny amount of isolated Cr(III) species, does not change. This behavior indicates that in our experimental condition the Cr(III) sites are not involved in the polymerization of ethylene, as suggested by DR UV-Vis spectroscopy and in good agreement with the observation that the amount of Cr(III) species does not correlate with the polymerization activity (Figure S1 and Figure S3).

4. Discussion

A systematic investigation on the effect of TEAl on the Cr(VI)/SiO_2 Phillips catalyst was carried out by combining the results of kinetic tests during the polymerization of ethylene, spectroscopic techniques (DR UV-Vis-NIR, EPR, FT-IR of probe molecules) aimed at elucidating the properties of the modified Cr sites, and the polymer characterization. We proved that TEAl eliminates the induction time and greatly accelerates the initiation rate of ethylene polymerization, in good agreement with the previous observations.[2] This suggests that TEAl reduces (and probably alkylates) at least a fraction of the Cr(VI) sites, which become rapidly reactive toward the polymerization of ethylene, thus making ethylene self-alkylation dispensable. Moreover, the obtained PE differs from that produced with an unmodified Cr(VI)/SiO_2 catalyst, especially in terms of M_w (which is higher) and M_w/M_n (which is broader and shows a visible tail also at low-M_w). These results clearly indicate that TEAl generates a large variety of modified Cr sites, each one responsible for the production of polymer chains with different molecular weight.

Elucidating the properties of the modified Cr sites at a molecular level was the next and very challenging target. According to FT-IR, DR UV-Vis-NIR and EPR spectroscopies, only ca. 50% of the original Cr(VI) sites are reduced at an Al:Cr ratio of 2:1. Highly coordinated Cr(II) and Cr(III) sites are both present in the modified catalyst, as previously suggested by Cicmil et al.[9,27,28] The 6-fold coordination of these sites is largely justified by the presence of $–OAlR_2$ moieties at the silica surface (from reaction of TEAl with silanols and siloxane groups), as well as by the presence of $Al(OR)_xR_y$ by-products. All these Al-containing species are detected by FT-IR spectroscopy, although they cannot be distinguished, and a fraction of them is coordinatively unsaturated and can be probed by CD_3CN, which is an excellent probe for Lewis acid sites. Besides Cr(II) and Cr(III) sites, however, we also claim the presence of a substantial fraction of alkylated Cr(IV) sites, which are EPR silent but observable by DR UV-Vis-NIR, although they cannot be quantified since their contribution overlaps with that of the remaining mono-chromates. The existence of Cr(IV) bis-alkylated sites, formed through steps 1 and 2 in Scheme 1, have been previously discussed by Mc Daniel [2]

As far as the accessibility of the Cr sites is concerned, we tested it by using CO and CD_3CN as probe molecules, the former being very sensitive to the molecular site structure, and the latter to their acidic character. The Cr(III) sites seem not accessible, probably because they are largely covered by the Al-containing fragments. The Cr(IV) bis-alkyl sites are probed by CO, which inserts into the Cr-C bond to give Cr-acyl complexes. Finally, the Cr(II) sites are accessible

to both CO and CD_3CN. CO incontrovertibly indicates that the Cr(II) sites are not bis-grafted (as for the CO-reduced Phillips catalyst), but rather mono-grafted as ≡Si-O-Cr(II)-L sites (where L = alkyl). They likely derive from the over-reduction of the Cr(IV) bis-alkyl species, following step 3 in Scheme 1, and they are stabilized by flexible ligands nearby, such as ≡Si-OAlR_2 (or similar) moieties, and this is the reason why they appear as highly coordinated in the UV-Vis spectra. Correspondingly, CD_3CN reveals the presence of a certain fraction of Cr(II)···Al(III) bi-metallic couples in sufficient close proximity to bind a CD_3CN molecule in a bridge fashion, which behave as strong Lewis acid sites.

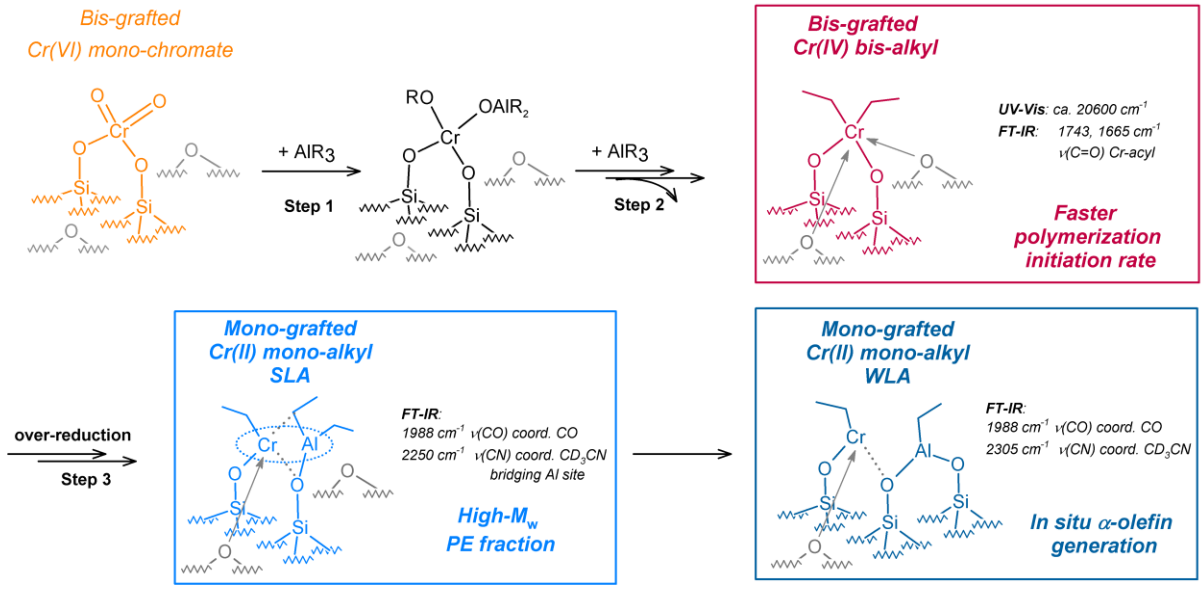

Scheme 1. Representation of the structure at a molecular level of the Cr species detected by spectroscopic methods on Cr(VI)/SiO_2+TEAl(2:1). To these species we should add 6-fold coordinated Cr(III), which have been detected by EPR and DR UV-Vis, but we have no additional indication helping in the definition of their structure. The main spectroscopic fingerprints and the contribution of each Cr species to the obtained PE are also reported. WLA = weak Lewis acid; SLA = strong Lewis acid. The dotted circle indicates a close proximity between the mono-grafted Cr(II) species and the Al-containing moiety.

Scheme 1 schematically shows the main Cr species assumed so far to be formed starting from Cr(VI)/SiO_2 + TEAl. Their main spectroscopic fingerprints have been determined in this work. Additionally, isolated Cr(III) sites have been detected by EPR and DR UV-Vis, which, however, probably do not participate in the reaction. Plausibly, all of these sites could play a role in the polymerization of ethylene. However, the bis-grafted Cr(IV) bis-alkyl species seem to be the major actors (as demonstrated by UV-Vis performed during the early stages of ethylene polymerization), since alkylation made them already prone to insert ethylene. Their presence explains the faster polymerization initiation rate. On the basis of previous literature,[2,38,39] we can advocate the mono-grafted Cr(II) sites with weak Lewis acid properties (WLA) as responsible for in situ α-olefin generation. Hence, they contribute with the enchainment of short polymer branches, concurring to the reduced PE crystallinity and the relatively low melting temperature. The presence of a certain amount of mono-grafted Cr(II) sites with a strong Lewis acidic character (SLA) probably accounts for the formation of the high-M_w polymer fraction, since it has been already demonstrated that Cr(II) sites with increased acidity afford a PE with a higher molecular weight.[73] Finally, as far as the polymer fraction with low molecular

weight is concerned, this might be due to the occurrence of a chain-termination through an alkyl exchange between the growing polymer chains and the Al-alkyl excess,[2] contributing to broaden the M_w/M_n to the low-M_W side. Another possible explanation to account for the low-M_w fraction formed with Cr(VI)/SiO_2 + TEAl is that higher polymerization initiation rate, the more the polymerization will be exothermic, determining the catalyst particle to initially overheat and hence producing the low-M_w polymer fraction.

Conclusions

All in all, combining the whole set of spectroscopic data collected in this work with the polymerization tests and the characterization of the obtained PE, we did a step forward in the understanding of the role of Al-alkyls in modifying the Phillips catalyst. On one side, our data validate some of the hypothesis postulated in the past exclusively on the basis of the observation of the polymer. On the other side, they introduce innovative concepts that can be useful to improve the design of the Phillips catalyst on rational basis. In particular, we demonstrated that the catalytic performance of the Cr sites depend not only on the oxidation state, but rather on a combination of molecular structure, acidic character and nature of the ancillary ligands. The dominant role of Cr(IV) bis-alkylated sites in ethylene polymerization has strong mechanistic implications and suggests that similar species might be actually the active sites in unmodified Cr(II)/SiO_2 involved in the polymerization of ethylene. A self-alkylation mechanism involving the formation of Cr(IV) bis-alkyl sites starting from Cr(II) is also supported by the very recent work of McDaniel[74] and would be compatible with our recent experimental observations.[57] Indeed, we were not able to detect any EPR active species after the polymerization of ethylene over a Cr(II)/SiO_2 catalyst, a fact which seems to strengthen the role of partially reduced but non-paramagnetic Cr sites in the polymerization.

Finally, we confirmed once more that mono-grafted Cr sites are involved in the oligomerization of ethylene, as suggested by Mc Daniel,[2] but we also found that this is not sufficient. The mono-grafted Cr sites must also behave as weak Lewis acid sites. On the other hand, Cr sites with a strong Lewis acid character likely produce PE with a very high molecular weight, irrespective of their local structure. It is thus clear that, by tuning the structure and the acid character of the Cr sites, it is possible to move from a system that essentially affords oligomers from ethylene to one that affords high M_w polymers. Overall, these conclusions can be useful in designing Cr-based catalysts not only for ethylene polymerization but also for ethylene oligomerization.

References

(1) Hogan, J. P.; Banks, R. L., Polymers and production thereof, U.S. Patent 2, 825, 721, 1958.

(2) McDaniel, M. P., A Review of the Phillips Supported Chromium Catalyst and Its Commercial Use for Ethylene Polymerization, *Adv. Catal.* **2010**, *53*, 123-606.

(3) McDaniel, M. P., *Handbook of heterogeneous catalysis*, in: Handbook of heterogeneous catalysis; Ertl, G.; Knözinger, H.; Weitkamp, J., Ed.; VHC: Weinheim, **1997**; Vol. 5, p. 2400.

(4) McDaniel, M. P.; Witt, D. R.; Benham, E. A., Effect of alkali metal doping on the performance of Cr/silica catalysts in ethylene polymerization, *J. Catal.* **1998**, *176*, 344-351.

(5) McDaniel, M. P., Influence of porosity on PE molecular weight from the Phillips Cr/silica catalyst, *J. Catal.* **2009**, *261*, 34–49.

(6) McDaniel, M., Some reflections on the current state of Cr-based polymerization catalysts, *MRS Bulletin* **2013**, *38*, 234-238.

(7) McDaniel, M., Manipulating polymerization chemistry of Cr/silica catalysts through calcination, *Appl. Catal. A* **2017**, *542*, 392-410.

(8) Jayaratne, K. C.; Cymbaluk, T. H.; Jensen, M. D., A Career in Catalysis: Max McDaniel, *ACS Catal.* **2018**, *8*, 602-614.

(9) Cicmil, D.; Meeuwissen, J.; Vantomme, A.; Wang, J.; van Ravenhorst, I. K.; van der Bij, H. E.; Munoz-Murillo, A.; Weckhuysen, B. M., Polyethylene with Reverse Co-monomer Incorporation: From an Industrial Serendipitous Discovery to Fundamental Understanding, *Angew. Chem.* **2015**, *54*, 13073-13079.

(10) Groppo, E.; Lamberti, C.; Bordiga, S.; Spoto, G.; Zecchina, A., The structure of active centers and the ethylene polymerization mechanism on the Cr/SiO_2 catalyst: a frontier for the characterization methods, *Chem. Rev.* **2005**, *105*, 115-183.

(11) Groppo, E.; Martino, G. A.; Piovano, A.; Barzan, C., The Active Sites in the Phillips Catalysts: Origins of a Lively Debate and a Vision for the Future, *ACS Catal.* **2018**, *8*, 10846-10863.

(12) Barzan, C.; Piovano, A.; Braglia, L.; Martino, G. A.; Lamberti, C.; Bordiga, S.; Groppo, E., Ligands Make the Difference! Molecular Insights into CrVI/SiO2 Phillips Catalyst during Ethylene Polymerization, *J. Am. Chem. Soc.* **2017**, *139*, 17064-17073.

(13) Ghiotti, G.; Garrone, E.; Zecchina, A., IR investigation of polymerization centres of the Phillips catalyst, *J. Mol. Catal.* **1988**, *46*, 61-77.

(14) Myers, D. L.; Lunsford, J. H., Silica-supported chromium catalysts for ethylene polymerization: the active oxidation states of chromium, *J. Catal.* **1986**, *99*, 140-148.

(15) Weckhuysen, B. M.; Verberckmoes, A. A.; Buttiens, A. L.; Schoonheydt, R. A., Diffuse-reflectance spectroscopy study of the thermal genesis and molecular structure of chromium supported catalysts, *J. Phys. Chem.* **1994**, *98*, 579-584.

(16) Liu, B.; Šindelář, P.; Fang, Y.; Hasebe, K.; Terano, M., Correlation of oxidation states of surface chromium species with ethylene polymerization activity for Phillips CrOx/SiO2 catalysts modified by Al-alkyl cocatalyst, *J Mol Catal A Chem* **2005**, *238*, 142-150.

(17) Conley, M. P.; Delley, M. F.; Siddiqi, G.; Lapadula, G.; Norsic, S.; Monteil, V.; Safonova, O. V.; Copéret, C., Polymerization of ethylene by silica-supported dinuclear CrIII sites through an initiation step involving C=H bond activation, *Angew. Chem. Int. Ed.* **2014**, *53*, 1872-1876.

(18) Delley, M. F.; Conley, M. P.; Copéret, C., Polymerization on CO-reduced Phillips catalyst initiates through the C-H bond activation of ethylene on Cr-O sites, *Catal Lett* **2014**, *144*, 805-808.

(19) Delley, M. F.; Núñez-Zarur, F.; Conley, M. P.; Comas-Vives, A.; Siddiqi, G.; Norsic, S.; Monteil, V.; Safonova, O. V.; Copéret, C., Proton transfers are key elementary steps in ethylene polymerization on isolated chromium(III) silicates, *Proc. Natl. Acad. Sci. U. S. A.* **2014**, *111*, 11624-11629.

(20) Jehng, J. M.; Wachs, I. E.; Weckhuysen, B. M.; Schoonheydt, R. A., Surface-chemistry of silica-titania-supported chromium-oxide catalysts, *J. Chem. Soc. Faraday Trans.* **1995**, *91*, 953-961.

(21) Phillips Cr/silica catalyst for ethylene polymerization.

(22) Fong, A.; Yuan, Y.; Ivry, S. L.; Scott, S. L.; Peters, B., Computational kinetic discrimination of ethylene polymerization mechanisms for the Phillips (Cr/SiO<inf>2</inf>) catalyst, *ACS Catal.* **2015**, *5*, 3360-3374.

(23) Fong, A.; Peters, B.; Scott, S. L., One-Electron-Redox Activation of the Reduced Phillips Polymerization Catalyst, via Alkylchromium(IV) Homolysis: A Computational Assessment, *ACS Catal.* **2016**, *6*, 6073-6085.
(24) Liu, H.; Fang, Y.; Nakatani, H.; Terano, M., Surface physico-chemical state of CO-prereduced Phillips CrO x/SiO2 catalyst and unique polymerization behavior in the presence of Al-alkyl cocatalyst, *Macromol Symp.* **2004**, *213*, 37-46.
(25) Xia, W.; Liu, B.; Fang, Y.; Hasebe, K.; Terano, M., Unique polymerization kinetics obtained from simultaneous interaction of Phillips Cr(VI)Ox/SiO2 catalyst with Al-alkyl cocatalyst and ethylene monomer, *J Mol Catal A Chem* **2006**, *256*, 301-308.
(26) Xia, W.; Tonosaki, K.; Taniike, T.; Terano, M.; Fujitani, T.; Liu, B. P., Copolymerization of Ethylene and Cyclopentene with the Phillips CrOx/SiO2 Catalyst in the Presence of an Aluminum Alkyl Cocatalyst, *J. Appl. Polym. Sci.* **2009**, *111*, 1869–1877.
(27) Cicmil, D.; Meeuwissen, J.; Vantomme, A.; Weckhuysen, B. M., Real-time Analysis of a Working Triethylaluminium-Modified Cr/Ti/SiO2 Ethylene Polymerization Catalyst with In Situ Infrared Spectroscopy, *ChemCatChem* **2016**, *8*, 1937-1944.
(28) Cicmil, D.; van Ravenhorst, I. K.; Meeuwissen, J.; Vantomme, A.; Weckhuysen, B. M., Structure-performance relationships of Cr/Ti/SiO2 catalysts modified with TEAl for oligomerisation of ethylene: tuning the selectivity towards 1-hexene, *Catal Sci Technol* **2016**, *6*, 731-743.
(29) Bent, B. E.; Nuzzo, R. G.; Dubois, L. H., Surface Organometallic Chemistry in the Chemical Vapor Deposition of Aluminum Films Using Triisobutylaluminum: Hydride and ,Alkyl Elimination Reactions of Surface Alkyl Intermediates, *J. Am. Chem. Soc.* **1989**, *111* 1634.
(30) Klepper, K. B.; Nilsen, O.; Fjellvåg, H., Deposition of thin films of organic–inorganic hybrid materials based on aromatic carboxylic acids by atomic layer deposition, *Dalton Trans.* **2010**, *39*, 11628.
(31) Kerber, R. N.; Kermagoret, A.; Callens, E.; Florian, P.; Massiot, D.; Lesage, A.; Coperet, C.; Delbecq, F.; Rozanska, X.; Sautet, P., Nature and Structure of Aluminum Surface Sites Grafted on Silica from a Combination of High-Field Aluminum-27 Solid-State NMR Spectroscopy and First-Principles Calculations, *J. Am. Chem. Soc.* **2012**, *134*, 6767-6775.
(32) Li, J. H.; DiVerdi, J. A.; Maciel, G. E., Chemistry of the silica surface: Liquid-solid reactions of silica gel with trimethylaluminum, *J. Am. Chem. Soc.* **2006**, *128*, 17093-17101.
(33) Pelletier, J.; Espinas, J.; Vu, N.; Norsic, S.; Baudouin, A.; Delevoye, L.; Trebosc, J.; Le Roux, E.; Santini, C.; Basset, J.-M.; Gauvin, R. M.; Taoufik, M., A well-defined silica-supported aluminium alkyl through an unprecedented, consecutive two-step protonolysis–alkyl transfer mechanism, *Chem. Commun.* **2011**, *47*, 2979.
(34) Martino, G. A.; Piovano, A.; Barzan, C.; Bordiga, S.; Groppo, E., The Effect of Al-Alkyls on the Phillips Catalyst for Ethylene Polymerization: The Case of Diethylaluminum Ethoxide (DEALE), *Top. Catal.* **2018**, *61*, 1465-1473.
(35) Hogan, J. P., Polymerization of olefins U.S. Patent 3,878,179, 1975.
(36) Witt, D. R., Supported chromium oxide catalyst having mixed adjuvant U.S. Patent 3,947,433, 1976.
(37) Bergmeister, J. J.; Wolfe, A. R.; Secora, S. J.; Benham, E. A.; Coutant, W. R.; McDaniel, M. P., U.S. Patent 6,174,981, 2001.
(38) Barzan, C.; Groppo, E.; Quadrelli, E. A.; Monteil, V.; Bordiga, S., Ethylene polymerization on a SiH_4-modified Phillips catalyst: detection of in situ produced a-olefins by operando FT-IR spectroscopy, *Phys.Chem.Chem.Phys.* **2012**, *14*, 2239–2245.
(39) Barzan, C.; Gianolio, D.; Groppo, E.; Lamberti, C.; Monteil, V.; Quadrelli, E. A.; Bordiga, S., The effect of hydrosilanes on the active sites of the phillips catalyst: The secret for in situ olefin generation, *Chem. Eur. J.* **2013**, *19*, 17277-17282.
(40) Groppo, E.; Seenivasan, K.; Barzan, C., The potential of spectroscopic methods applied to heterogeneous catalysts for olefin polymerization, *Catal. Sci. Technol.* **2013**, *3*, 858-878.
(41) Groppo, E.; Damin, A.; Otero Arean, C.; Zecchina, A., Enhancing the Initial Rate of Polymerisation of the Reduced Phillips Catalyst by One Order of Magnitude, *Chem. Eur. J.* **2011**, *17*, 11110 – 11114.

(42) The temperature of 150 °C adopted in this work is slightly higher with respect that used in industrial conditions. This correction was necessary to compensate for the low ethylene pressure employed in our experimental conditions.
(43) Kissin, Y. V.; Brandolini, A. J.; Garlick, J. L., Kinetics of ethylene polymerization reactions with chromium oxide catalysts, *J. Polym. Sci. A* **2008**, *46*, 5315-5329.
(44) Demmelmaier, C. A.; White, R. E.; van Bokhoven, J. A.; Scottt, S. L., Nature of $SiOCrO_2Cl$ and $(SiO)_2CrO_2$ sites prepared by grafting CrO_2Cl_2 onto silica, *J. Phys. Chem. C* **2008**, *112*, 6439-6449.
(45) Demmelmaier, C. A.; White, R. E.; van Bokhoven, J. A.; Scott, S. L., Evidence for a chromasiloxane ring size effect in Phillips (Cr/SiO_2) polymerization catalysts, *J. Catal.* **2009**, *262*, 44-56.
(46) Kvisle, S.; Rytter, E., Infrared matrix isolation spectroscopy of trimethylgallium, trimethylaluminium and triethylaluminium, *Spectrochim. Acta, Part A* **1984**, *40*, 939-951.
(47) Kuzuba, Y.; Monoi, T.; Matsumoto, R.; Ogawa, K.; Kanazawa, S.; Hattori, T., EP 2447287 B1, 2017.
(48) Weckhuysen, B. M.; Wachs, I. E.; Shoonheydt, R. A., Surface chemistry and spectroscopy of chromium in inorganic oxides, *Chem. Rev.* **1996**, *96*, 3327-3349.
(49) Weckhuysen, B. M.; Deridder, L. M.; Grobet, P. J.; Schoonheydt, R. A., Redox behavior and dispersion of supported chromium catalysts, *J. Phys. Chem.* **1995**, *99*, 320-326.
(50) Weckhuysen, B. M.; Deridder, L. M.; Schoonheydt, R. A., A quantitative diffuse reflectance spectroscopy study of supported chromium catalysts, *J. Phys. Chem.* **1993**, *97*, 4756-4763.
(51) Weckhuysen, B. M.; Schoonheydt, R. A.; Jehng, J. M.; Wachs, I. E.; Cho, S. J.; Ryoo, R.; Kijlstra, S.; Poels, E., Combined DRS-RS-EXAFS-XANES-TPR study of supported chromium catalysts, *J. Chem. Soc. Faraday Trans.* **1995**, *91*, 3245-3253.
(52) Cordischi, D.; Indovina, V.; Occhiuzzi, M., Exchange-coupled Cr(V) and Mo(V) Ions on the surface of CrO_x ZrO_2 and MoO_x ZrO_2 - an electron-paramagnetic resonance study, *J. Chem. Soc. Faraday Trans.* **1991**, *87*, 3443-3447.
(53) Cordischi, D.; Indovina, V.; Occhiuzzi, M., The dispersion of Cr(V) and Mo(V) on the surface of various oxides, as investigated by ESR spectroscopy, *Appl. Surf. Sci.* **1992**, *55*, 233-237.
(54) Cordischi, D.; Campa, M. C.; Indovina, V.; Occhiuzzi, M., Structure of Cr-V species on the surface of various oxides - Reactivity with NH_3 and H_{2O}, as investigated by EPR spectroscopy, *J. Chem. Soc. Faraday Trans.* **1994**, *90*, 207-212.
(55) Groeneveld, C.; Wittgen, P. P. M. M.; Kersbergen van, A. M.; Hestrom, P. L. M.; Nuijten, C. E.; Schuit, G. C. A., *J. Catal.* **1979**, *59*, 153.
(56) Weckhuysen, B. M.; Schoonheydt, R. A.; Mabbs, F. E.; Collison, D., Electron paramagnetic resonance of heterogeneous chromium catalysts, *J. Chem. Soc. Faraday Trans.* **1996**, *92*, 2431-2436.
(57) Morra, E.; Martino, G. A.; Piovano, A.; Barzan, C.; Groppo, E.; Chiesa, M., In Situ X- and Q-Band EPR Investigation of Ethylene Polymerization on Cr/SiO2 Phillips Catalyst, *J. Phys. Chem. C* **2018**, *122*, 21531-21536.
(58) Mowat, W.; Shortland, A. J.; Hill, N. J.; Wilkinson, G., Elimination stabilized alkyls. Part II. Neopentyl and related alkyls of chromium(IV), *J. Chem. Soc. Dalton Trans.* **1973** 770-778.
(59) Amor Nait Ajjou, J.; Scott, S. L., Reactions of tetraalkylchromium(IV) with silica: Mechanism of grafting and characterization of surface organometallic complexes, *Organometallics* **1997**, *16*, 86-92.
(60) Lamberti, C.; Zecchina, A.; Groppo, E.; Bordiga, S., Probing the surfaces of heterogeneous catalysts by in situ IR spectroscopy, *Chem. Soc. Rev.* **2010**, *39*, 4951–5001.
(61) Knoezinger, H.; Krietenbrink, H., Infrared spectroscopic study of the adsorption of nitriles on aluminium oxide. Fermi resonance in coordinated acetonitrile, *J. Chem. Soc., Faraday Trans. 1,* **1975**, *71*, 2421-2430.
(62) Morterra, C.; Mentruit, M. P.; Cerrato, G., Acetonitrile adsorption as an IR spectroscopic probe for surface acidity/basicity of pure and modified zirconias, *PCCP* **2002**, *4*, 676-687.
(63) Morterra, C.; Cerrato, G.; Novarino, E.; Mentruit, M. P., On the adsorption of acetonitrile on pure and sulfated tetragonal zirconia (t-ZrO2), *Langmuir* **2003**, *19*, 5708-5721.
(64) Platero, E. E.; Mentruit, M. P.; Morterra, C., Fourier transform infrared spectroscopy study of CD3CN adsorbed on pure and doped gamma-alumina, *Langmuir* **1999**, *15*, 5079-5087.

(65) Cerruti, M.; Bolis, V.; Magnacca, G.; Morterra, C., Surface chemical functionalities in bioactive glasses. The gas/solid adsorption of acetonitrile, *PCCP* **2004**, *6*, 2468-2479.
(66) Busca, G., Acid catalysts in industrial hydrocarbon chemistry, *Chem. Rev.* **2007**, *107*, 5366-5410.
(67) Busca, G., Bases and Basic Materials in Chemical and Environmental Processes. Liquid versus Solid Basicity, *Chem. Rev.* **2010**, *110*, 2217-2249.
(68) Zecchina, A.; Scarano, D.; Bordiga, S.; Spoto, G.; Lamberti, C., Surface structures of oxides and halides and their relationships to catalytic properties, *Adv. Catal.* **2001**, *46*, 265-397 and references therein.
(69) Calderazzo, F., Synthetic and Mechanistic Aspects of Inorganic Insertion Reactions. Insertion of Carbon Monoxide, *Angew. Chem. -Int. Edit.* **1977**, *16*, 299-311.
(70) Calderazzo, F., Synthesis and properties of transition metal to carbon bonds, *Pure Appl. Chem.* **1973**, *33*, 453-474.
(71) Hitam, R. B.; Narayanaswamy, R.; Rest, A. J., Matrix isolation studies of the bonding of acetyl groups in the co-ordinatively unsaturated species acetyltetracarbonylmanganese and acetylmonocarbonyl(η-cyclopentadienyl)iron, *J.Chem. Soc., Dalton Trans.* **1983** 615-618.
(72) Barnett, K. W.; Beach, D. L.; Gaydos, S. P.; Pollmann, T. G., Methyl and acetyl complexes of chromium and tungsten. Observations on metal—carbon bond strength variations in the chromium triad, *J.Organomet. Chem.* **1974**, *69*, 121-130.
(73) Martino, G. A.; Barzan, C.; Piovano, A.; Budnyk, A.; Groppo, E., Tracking the reasons for the peculiarity of Cr/Al2O3 catalyst in ethylene polymerization, *J. Catal.* **2018**, *357*, 206-212.
(74) Cruz, C. A.; Monwar, M. M.; Barr, J.; McDaniel, M. P., Identification of the Starting Group on the First PE Chain Produced by the Phillips Catalyst, *Macromolecules* **2019** 10.1021/acs.macromol.1029b00588.

SUPPORTING INFORMATION

Rationalizing the effect of triethyl-aluminum on the Cr/SiO_2 Phillips catalysts

Giorgia A. Martino,[1] Alessandro Piovano,[1] Caterina Barzan,[1] Jabor Rabeah,[2] Giovanni Agostini,[2,#] Angelika Bruekner,[2] Giuseppe Leone[3], Giorgia Zanchin,[3] Takashi Monoi,[4] and Elena Groppo[1,*]

[1]Department of Chemistry, NIS Centre and INSTM, University of Torino, via G. Quarello 15A, 10135 Torino, Italy
[2] Leibniz Institute for Catalysis at the University of Rostock (LIKAT), Albert-Einstein-Str. 29D-18059 Rostock
[3] CNR-Istituto per lo Studio delle Macromolecole (ISMAC), via A. Corti 12, I-20133 Milano, Italy
*Corresponding author: elena.groppo@unito.it

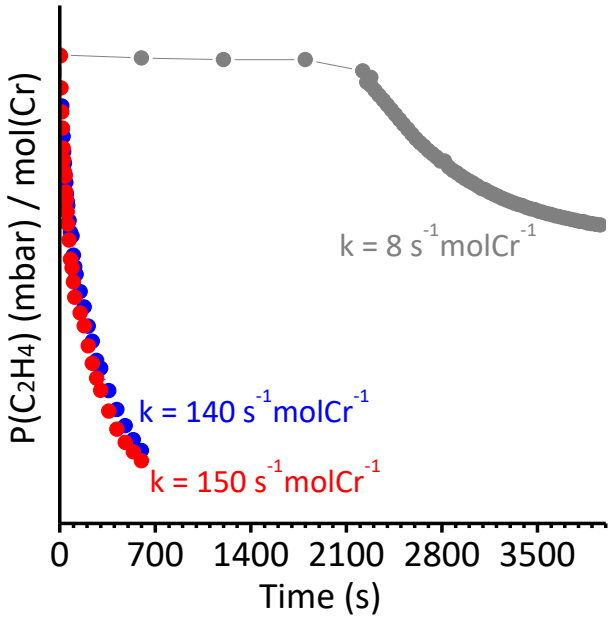

Figure S1. Kinetics of the gas-phase ethylene polymerization on the Cr(VI)/SiO_2 catalyst (grey) in comparison to that on Cr(VI)/SiO_2+TEAl(2:1) (blue), and on Cr(VI)/SiO_2+TEAl(4:1) (red). The rate constants k, evaluated during the first minute of reaction, are also indicated.

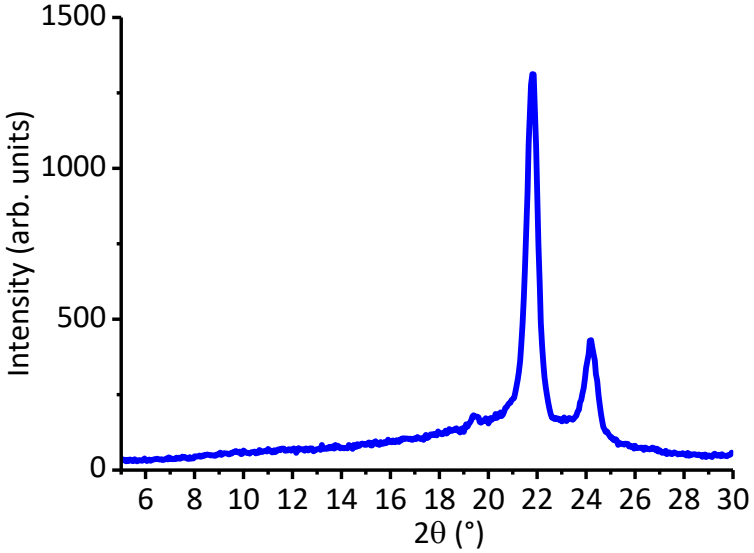

Figure S2. XRD pattern of the PE obtained over the Cr(VI)/SiO_2+TEAl(2:1) catalyst.

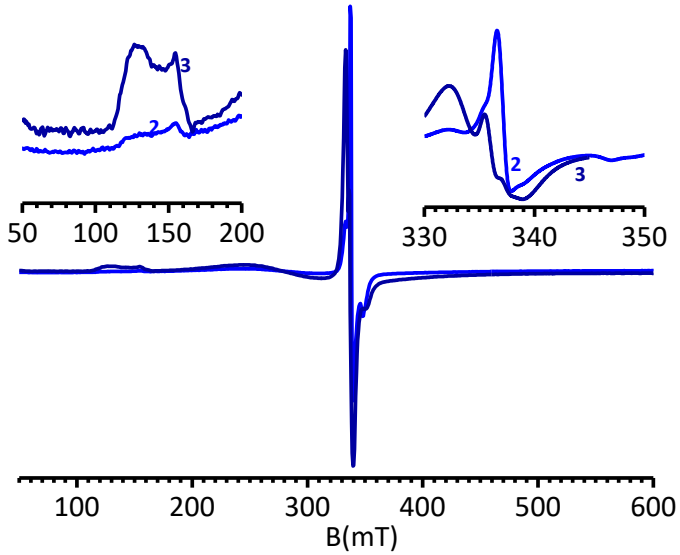

Figure S3. X-band EPR spectra (collected at 100 K) of Cr(VI)/SiO_2+TEAl(2:1) (curve 2) and Cr(VI)/SiO_2+TEAl(4:1) (curve 3).

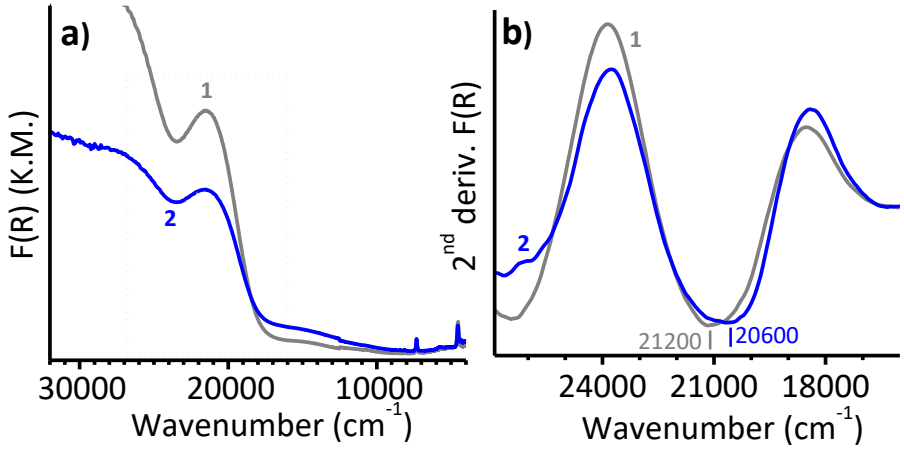

Figure S4. Part a): DR UV-Vis-NIR spectra of Cr(VI)/SiO_2 (spectra 1) and of Cr(VI)/SiO_2+TEAl(2:1) (spectra 2). Part b) the same spectra as part a) reported in terms of the second derivative in a magnified spectral region, in order to better highlight the shift of the band centered at ca. 21000 cm^{-1}.A maximum in the original spectrum becomes a minimum in the second derivative.

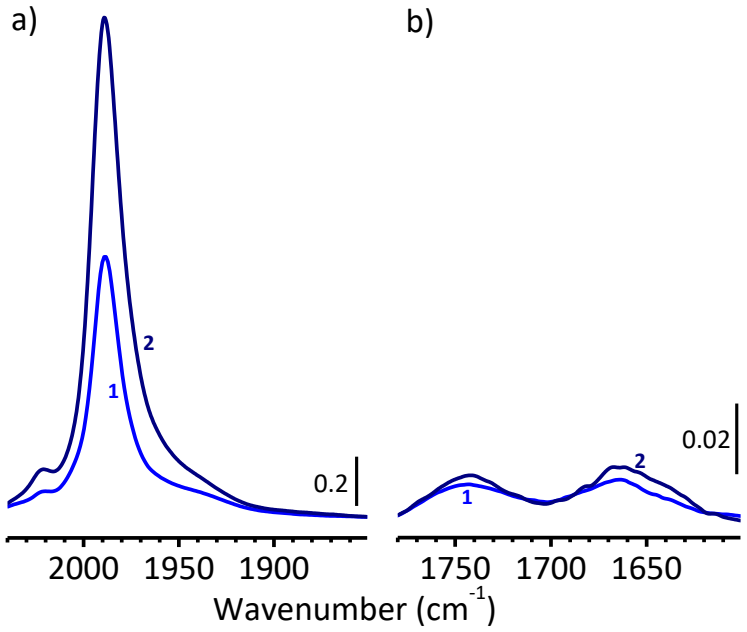

Figure S5. FT-IR spectra of CO adsorbed at room temperature on Cr(VI)/SiO_2+TEAl(2:1) (curve 1) and on Cr(VI)/SiO_2+TEAl(4:1) (curve 2). The spectra are normalized for the optical thickness of the pellet and for the CO equilibrium pressure, hence the absolute intensities are comparable. The spectra are vertically translated for clarity. Part a) shows the ν(C≡O) region of CO coordinated to reduced Cr sites, while part b) shows the to ν(C=O) region of Cr η^1-acyl complexes, which are formed by insertion of CO into a Cr-alkyl bond.

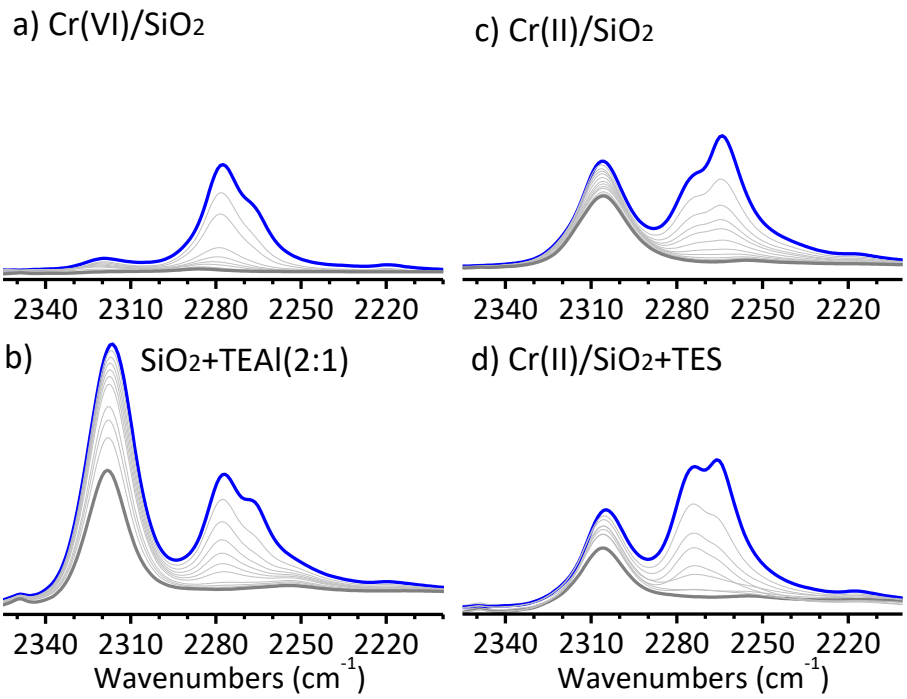

Figure S6. Evolution of the FT-IR spectra, in the ν̃(C≡N) region, for CD_3CN adsorbed at room temperature on Cr(VI)/SiO_2 (part a), SiO_2+TEAl(2:1) (part b), Cr(II)/SiO_2 (part c), and Cr(II)/SiO_2+TES (part d), as a function of the CD_3CN coverage (blue: maximum coverage, dark grey: irreversible fraction of CD_3CN, light grey: intermediate coverages).

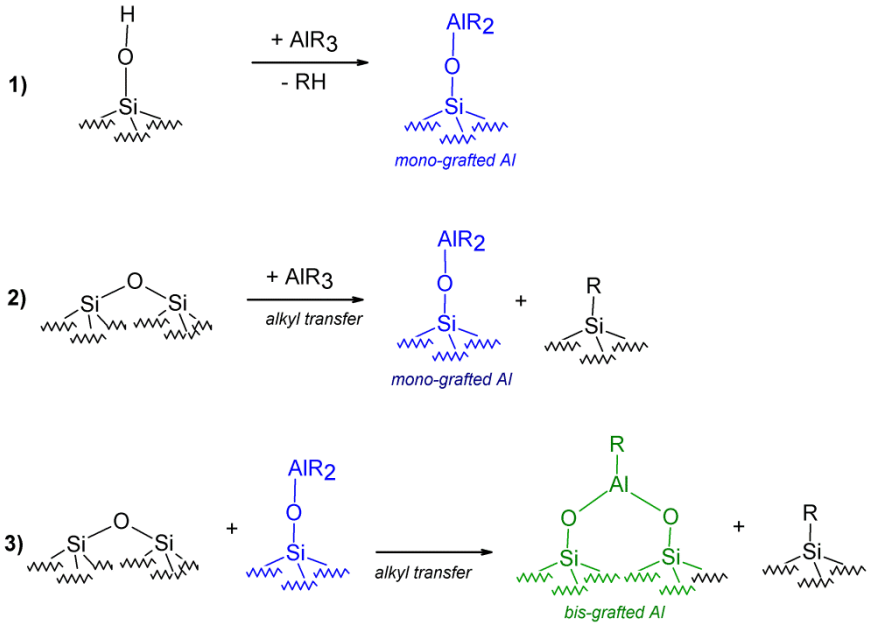

Scheme S1. Some of the surface structures that can be formed upon reaction of monomeric TEAl with the SiO_2 surface.